Published paper

Bryan, M.T., Dean, J., Schrefl, T., Thompson, F.E., Haycock, J., Allwood, D.A. (2010) *The effect of trapping superparamagnetic beads on domain wall motion*, Applied Physics Letters, 96 (19), Article no. 192503
http://dx.doi.org/10.1063/1.3428775

The effect of trapping superparamagnetic beads on domain wall motion

Matthew T. Bryan,[1] Julian Dean,[1] Thomas Schrefl[1,2] Faye E. Thompson,[1] John Haycock,[3] and Dan A. Allwood[1]

[1] *Department of Engineering Materials, University of Sheffield, Portobello Street, Sheffield S1 3JD, UK*

[2] *St. Poelten University of Applied Sciences, 3100 St. Poelten, Austria*

[3] *The Kroto Research Institute, University of Sheffield, Sheffield S3 7HQ, UK*

Abstract

Domain walls may act as localized field sources to trap and move superparamagnetic beads for manipulating biological cells and DNA. The interaction between beads of various diameters and a wall is investigated using a combination of micromagnetic and analytical models. Domain walls can transport beads under applied magnetic fields, but the mutual attraction between the bead and wall causes drag forces affecting the bead to couple into the wall motion. Therefore, the interaction with the bead causes a fundamental change in the domain wall dynamics, reducing the wall mobility by five orders of magnitude.

Superparamagnetic beads are widely used within bioscience to separate, organize and manipulate biomolecules and cells,[1-6] and have promising clinical applications as they can be used as MRI contrast agents and in magnetic hyperthermia for the treatment of cancer.[7,8] Typically, they consist of iron oxide (Fe_2O_3 or Fe_3O_4) nanoparticles embedded in a polymer matrix, which may have an outer coating functionalized for a particular biological application. For example, coating the beads with monoclonal antibodies enables the beads to bind to cancer cells, allowing targeted magnetic hyperthermia.[9] The force due to an externally applied magnetic field on a superparamagnetic bead below saturation conditions is proportional to both the magnetic field strength and the field gradient. This has recently been exploited by devices that manipulate beads using stray fields from localized field sources such as closure domains of patterned elements[4,10,11] or domain walls in nanowires.[5,6,12,13] If the beads are attached to cells, the use of nanostructures enables the alignment or pattering of cells,[6] providing a fundamental control over cellular organization, which could generate future tissue engineering applications. In addition, domain walls may be propagated using applied magnetic fields or spin-polarized currents, so biological material attached to the beads can be translated over a pre-defined path. As nanowires can be patterned into sometimes quite complex networks,[14] this technique could significantly increase control over spatially-dependent interactions between biomolecules and cells. Domain walls are known to be pinned by beads that have bonded with the surface.[12] Unbonded beads have been shown to move with domain walls,[13] but the effect on the wall motion due to the loading of the bead has not been examined.

Here, micromagnetic and analytical modeling is used to examine the dynamic behavior of a system in which a superparamagnetic bead and head-to-head domain wall in a planar magnetic nanowire are coupled magnetostatically (Fig.1). Direct simulation of a domain wall dragging a bead is not possible using a micromagnetic solver, due to the need to include the effect of hydrodynamics on the bead motion. Instead, micromagnetic modelling is used to study the behavior of a wall around a stationary bead, representing the dynamic equilibrium state that is reached during wall movement, and then an analytical approach is adopted to show how hydrodynamic drag on the bead affects the wall velocity.

The micromagnetic model uses a finite element/boundary element method to solve the Landau-Liftshitz-Gilbert equation on 5 nm tetrahedral mesh. The nanowire is 100 nm wide, 5 nm thick and is assigned materials constants appropriate for $Ni_{81}Fe_{19}$ (Permalloy; Gilbert damping constant, α = 0.01; exchange stiffness constant, A = 1.3×10^{-11} Jm^{-1}; magneto-crystalline anisotropy, K = 0 Jm^{-3}; saturation magnetization, M_s = 800 kAm^{-1}). The bead has diameter d = 10 nm, 25 nm and 50 nm and has similar magnetic properties except that the saturation magnetization is 320 kAm^{-1}, similar to commercially available superparamagnetic beads (Spherotech CM-10-10). These properties ensure that each bead is single domain and aligns magnetically with the local magnetic field from the domain wall, so it is a reasonable model of a superparamagnetic particle. The domain wall was initialized at x = 0 nm, with the bead 10 nm above it (Fig. 1), before the system was allowed to relax to the minimum energy state. The domain wall, magnetized in the +y-direction, has a characteristic shape, with the widest section at y = 50 nm and the narrowest section at y = -50 nm

(Fig. 1c). To test the strength of the wall-bead coupling, progressively stronger fields were applied along the wire axis until the domain wall depinned from the bead.

Figure 2a shows dependence of the domain wall depinning field, H_{depin}, on the y-position of the d = 25 nm bead. The depinning field is strongest at just above 1200 Am^{-1} when the bead is above the widest section of the domain wall (y = 50 nm), plateaus at around 880 Am^{-1} above the wall centre and drops to 620 Am^{-1} above the narrowest section of the domain wall (y = -50 nm). When the bead is not directly above the wire H_{depin} drops sharply. The asymmetry in H_{depin} along the y-axis occurs because the bead-wall interaction is proportional to the field, which is asymmetric due to the smaller magnetic charge (magnetic pole density) distribution in the narrowest section of the wall.[15] Figure 2a also shows that the minimum energy of the system occurs around y = 50 nm. This suggests that beads attracted towards the domain wall are most likely to be found at positions that cause the most pinning.

Figure 2b shows how the depinning field at y = 50 nm varies with the bead diameter. Due to demagnetization fields within the wire there was a small (160 Am^{-1}) asymmetry between H_{depin} in the positive and negative x-directions, so Fig. 2b plots the average values. The depinning field is very sensitive to the bead diameter, following an approximately d^2 fit. The pinning on the wall may be related to the number of magnetic charges on the surface of the bead, which will also have a quadratic dependence on the bead diameter.

Applied fields below H_{depin} cause the wall to shift within the potential of the bead without significantly altering the wall structure (Fig. 1c). Figure 3a shows that the

wall displacement is approximately proportional to the applied field, although some cubic non-linearity is present, possibly due to the effect of the magnetostatic field from the bead. Demagnetization fields in the wire introduce an asymmetry of the wall position with respect to the applied field direction. Displacements from the equilibrium position generate energy gradients that attract the wall towards the bead upon removal of the applied field. Thus the wall experiences an effective force due to the bead. The reciprocal of this effect, where a fixed domain wall attracts a bead, has been seen experimentally.[13] In a homogeneous applied field, the interaction force acting on the wall is given by the change in the exchange and demagnetization energies with the relative positions of the bead and the wall. The force acting on the wall is analogous to a harmonic oscillator in that it is always directed towards the bead and proportional to its displacement (Fig. 3b). As a consequence, the interaction force on the wall, F_{bw}, has the form $F_{bw} = -kH$ (Fig. 3c). Of course, the force that the bead exerts on the wall is equal and opposite to the force the wall exerts on the bead, F_{wb}. Linear fits from Fig. 3c show that the force constant k = 1.5 fN/(Am^{-1}), 1.1 fN/(Am^{-1}) and 1.5 fN/(Am^{-1}) for the 10 nm, 25 nm and 50 nm diameter beads, respectively, suggesting that k is roughly independent of the bead size.

Further insight into the physical origin of the force constant k can be achieved by considering that the field exerts a pressure $2\mu_0 M_s H$ on the domain wall, where μ_0 is the permeability of free space. As the bead pins the wall, the effective force from the bead must cancel out the effective force from the pressure on the domain wall surface. This suggests that k can be described analytically as

$$k = 2\mu_0 M_S wT \qquad (1)$$

where w and T are the wire width and thickness, respectively. For the wire studied here, eq. (1) predicts k = 1 fN/(Am^{-1}), in reasonable agreement with the micromagnetically derived values.

In the above analysis, the bead is artificially fixed in the model, so the domain wall does not move along the wire for $H<H_{depin}$. If the bead is free to move, it will be towed under an applied field by the motion of the domain wall, provided the depinning field is not exceeded. When used for manipulation of biological material, the beads are surrounded by a carrier fluid. Therefore, the bead experiences not only the interaction force from the domain wall ($F_{wb} = kH$), but also a drag force from the fluid that it is suspended in. The drag force on a sphere can be found using Stoke's law: $F_{drag} = -6\pi\eta r v_b$, where η is the dynamic viscosity, r is the radius of the sphere and v_b is the bead velocity. Note that if the bead has interacted with biological material in the carrier fluid, for example if the bead is absorbed by a cell,[5] the sphere that the drag acts on may be larger than the bead alone. Friction between the bead and the surface is negligible, assuming that no chemical bonds form between the bead and the sample surface

The response of a domain wall to a field is characterized by the domain wall mobility, μ, which is defined by the ratio v_w/H, where v_w is the domain wall velocity. Due to the pinning from the bead, the bead and the wall move as a bound unit, so $v_w = v_b$. In general, this means a loaded wall will travel much slower than an unloaded wall under the same field. At dynamic equilibrium, the forces acting on the bead balance, so $F_{wb} + F_{drag} = 0$. Solving this for v_w/H, we find the effect of the hydrodynamic drag on the domain wall mobility

$$\mu = \frac{k}{6\pi\eta r} \tag{2}$$

where k can be described either using the micromagnetically derived force constants or by eq. (1). This is substantially different from the domain wall mobility below Walker breakdown when no bead is present: $\mu = \frac{\gamma_0 \Delta}{\alpha}$, where γ_0 is the is the gyromagnetic ratio and Δ is the domain wall width parameter.[16] For comparison, consider the effect of a 25 nm diameter bead in water ($\eta = 10^{-3}$ Pa.s) on wall motion in a 100 nm wide, 5 nm thick wire. Using the micromagnetically derived value of k, $\mu = 5\times10^{-6}$ m $s^{-1}/(Am^{-1})$. Without the bead, $\mu = 0.5$ m $s^{-1}/(Am^{-1})$. Therefore, it is likely that although free domain walls can travel at over 1 km.s^{-1},[17,18] domain walls loaded with superparamagnetic beads will move much slower. For example, at $H = 1200$ Am^{-1}, below the depinning field (Fig. 2b) and Walker breakdown field,[19] the bead-wall system will travel at 6 mm.s^{-1}. While this calculation does not consider the effect of bead aggregation or the increase in drag due to loading the beads with biological material, it suggests that domain walls can transport beads faster than has been demonstrated using transport of beads across arrays of magnetic elements (70 μm.s^{-1})[20] or in cell separation experiments (0.24 mm.s^{-1}).[21] Furthermore, as nanowires can be arbitrarily patterned, domain wall driven transport allows beads (and therefore attached biological material) to be positioned with much greater precision and selectivity than can be achieved using a global fluid flow. Such control could benefit cellular research, as signaling between cells may critically depend on the cell spacing.[22]

To summarize, micromagnetic and analytical models have shown that magnetic domain walls are pinned in the locality of superparamagnetic beads below a critical

magnetic field, proportional to the square of the bead diameter. The interaction causes the domain wall velocity to be limited by the hydrodynamic drag on the bead. Even from small beads, this effect is sufficient to reduce the domain wall mobility by five orders of magnitude. This suggests that beads transported using domain walls will travel far slower than suggested by velocity measurements on free domain walls.

[1] M. Tanase, E. J. Felton, D. S. Gray, A. Hultgren, C. S. Chen, and D. H. Reich, Lab Chip **5,** 598 (2005).
[2] J. P. Desai, A. Pillarisetti, and A. D. Brooks, Annu. Rev. Biomed. Eng. **9,** 35 (2007).
[3] D. W. Inglis, R. Riehn, J. C. Sturm, and R. H. Austin, J. Appl. Phys. **99,** 08K101 (2006).
[4] E. Mirowski, J. Moreland, S. Russek, M. Donahue, and K. W. Hsieh, J. Magn. Magn. Mater. **311,** 401 (2007).
[5] G. Vieira, T. Henighan, A. Chen, A. J. Hauser, F. Y. Yang, J. J. Chalmers, and R. Sooryakumar, Phys. Rev. Lett. **103,** 128101 (2009).
[6] M. T. Bryan, K. H. Smith, M. E. Real, M. A. Bashir, P. W. Fry, P. Fischer, M. Y. Im, T. Schrefl, D. A. Allwood, and J. W. Haycock, IEEE Magn. Lett. **1,** 1500104 (2010).
[7] Q. A. Pankhurst, N. K. T. Thanh, S. K. Jones, and J. Dobson, J. Phys. D-Appl. Phys. **42** (2009).
[8] Q. A. Pankhurst, J. Connolly, S. K. Jones, and J. Dobson, J. Phys. D-Appl. Phys. **36,** R167 (2003).
[9] S. J. DeNardo, G. L. DeNardo, L. A. Miers, A. Natarajan, A. R. Foreman, C. Gruettner, G. N. Adamson, and R. Ivkov, Clin. Cancer Res. **11,** 7087S (2005).
[10] E. Mirowski, J. Moreland, S. E. Russek, and M. J. Donahue, Appl. Phys. Lett. **84,** 1786 (2004).
[11] R. S. Conroy, G. Zabow, J. Moreland, and A. P. Koretsky, Appl. Phys. Lett. **93,** 203901 (2008).
[12] P. Vavassori, V. Metlushko, B. Ilic, M. Gobbi, M. Donolato, M. Cantoni, and R. Bertacco, Appl. Phys. Lett. **93,** 203502 (2008).
[13] P. Vavassori, M. Gobbi, M. Donolato, V. Metlushko, B. Ilic, M. Cantoni, D. Petti, S. Brivio, and R. Bertacco, in *arXiv:0903.3516v1 [physics.bio-ph]* (2009).
[14] D. A. Allwood, G. Xiong, C. C. Faulkner, D. Atkinson, D. Petit, and R. P. Cowburn, Science **309,** 1688 (2005).
[15] T. J. Hayward, M. T. Bryan, P. W. Fry, P. M. Fundi, M. R. J. Gibbs, D. A. Allwood, M. Y. Im, and P. Fischer, Phys. Rev. B **81,** 020410(R) (2010).
[16] M. T. Bryan, T. Schrefl, D. Atkinson, and D. A. Allwood, J. Appl. Phys **103,** 073906 (2008).
[17] D. Atkinson, D. A. Allwood, G. Xiong, M. D. Cooke, C. C. Faulkner, and R. P. Cowburn, Nature Mater. **2,** 85 (2003).
[18] S. Glathe, I. Berkov, T. Mikolajick, and R. Mattheis, Appl. Phys. Lett. **93,** 162505 (2008).
[19] M. T. Bryan, T. Schrefl, and D. A. Allwood, IEEE Trans. Magn. **46,** 1135 (2010).
[20] B. B. Yellen, O. Hovorka, and G. Friedman, Proc. Natl. Acad. Sci. U. S. A. **102,** 8860 (2005).
[21] D. W. Inglis, R. Riehn, R. H. Austin, and J. C. Sturm, Appl. Phys. Lett. **85,** 5093 (2004).
[22] C. J. Weijer, J. Cell Sci. **122,** 3215 (2009).

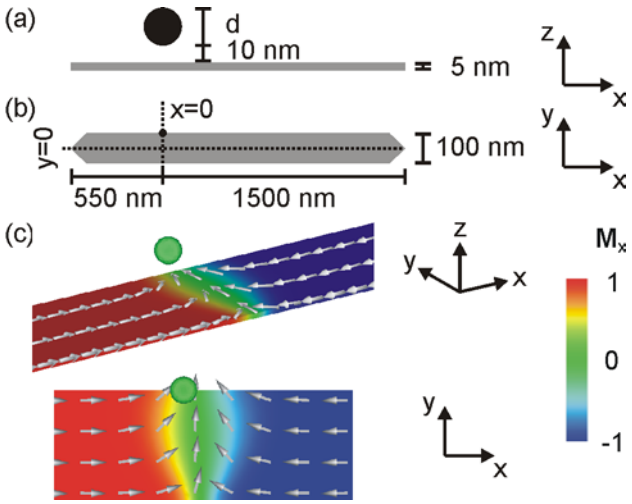

Figure 1: (a) Side view and (b) plan view schematic diagram of the system studied with bead of diameter, d (not to scale). (c) Micromagnetic calculation of a wall and bead (d = 25 nm) in a 400 Am^{-1} axial field. The arrows and the color scale indicate the total magnetization and the magnetization in the x-direction, M_x, respectively.

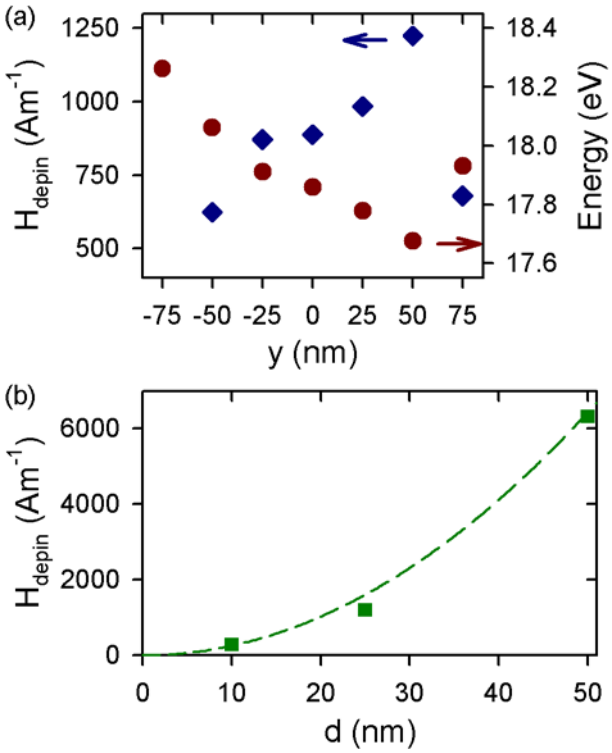

Figure 2: (a) The field required to depin the domain wall (H_{depin}) from a bead of diameter d = 25 nm and energy of the system at H = 0 Am^{-1} as a function of the y-coordinate of the bead centre at x = 0 nm. (b) H_{depin} as a function of d for beads positioned at x = 0 nm, y = 50 nm. The dashed line is a quadratic fit of the form $H_{depin} = 2.56d^2$.

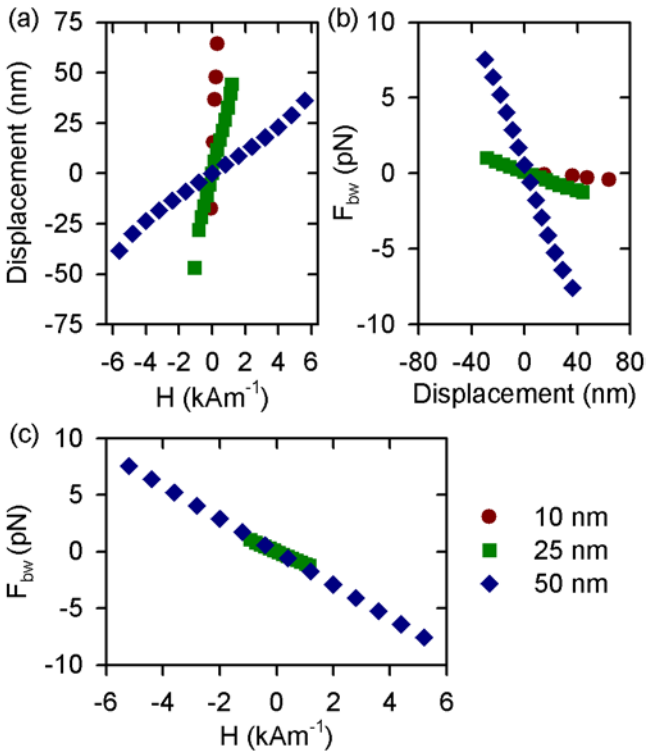

Figure 3: Micromagnetic calculations of (a) the effect of a magnetic field, H on the wall displacement relative to beads of diameter 10 nm, 25 nm and 50 nm, (b) the force from the bead on the wall, F_{bw}, as a function of the wall displacement, and (c) F_{bw} as a function of H.